Asian Journal of Electrical Sciences
ISSN: 2249-6297 (P) Vol.3 No.1, 2014, pp.23-34

DOI: https://doi.org/10.51983/ajes-2014.3.1.1916

Advanced Power Control Technique for Hybrid Wind-Solar Power GenerationSystem Used in Standalone Application

P.R. Syam Prasanth[1] and J.L. Sunil[2]

PG Scholar [1], Assistant Professor [2],

Department of EEE, Maria College of Engineering and Technology, Attoor, Tamilnadu, India

(Received on 10 march 2014 and accepted on 05 June 2014)

Abstract **- This paper proposes a unique standalone hybrid power generation system, applying advanced power control tech- niques, fed by four power sources: wind power, solar power, storage battery, and diesel engine generator, and which is not connected to a commercial power system. Considerable effort was put into the development of active-reactive power and dump power controls. The result of laboratory experiments revealed that amplitudes and phases of ac output voltage were well regulated in the proposed hybrid system. Different power sources can be interconnected anywhere on the same power line, leading to flex- ible system expansion. It is anticipated that this hybrid power generation system, into which natural energy is incorporated, will contribute to global environmental protection on isolated islands and in rural locations without any dependence on commercial power systems.**

Keyword **- Dump load, dump power control, low cost, stand-alone hybrid power generation system, storage battery.**

I. Introduction

Natural energy-based power generation systems are commonly equipped with storage batteries, to regulate output fluctuations resulting from natural energy variation. Therefore, it is necessary to prevent battery overcharging. As for the utility connected hybrid generation system consisting of a wind power, a solar power, and battery, the dump power is able to control to prevent overcharging the battery without dump load because of dump power transferred into the util-ity [1]. As for the individual power generation system, it is considered that a PV system featuring low-cost and simple control, which incorporates maximum power point tracking control that makes use of diode characteristics [2], or a PV system that features output stability with a multiple-input dc–dc converter capable of controlling the output of different power sources in combination [3], or a cascaded dc–dc converter PV system that features good efficiency along with low cost [4], or a wind turbine system that features output stability with a combination of an electric double-layer capacitor and storage battery [5], is suitable for use with hybrid power generation systems to stabilize power supply. In contrast, the standalone hybrid system is mainly composed of natural energy sources (i.e., wind power and solar power), and a storage battery; and in some cases, a diesel engine generator may be incorporated into the system as well. However, there is a tendency that the greater the system sophistication, the more suitable the power control techniques are required to be.

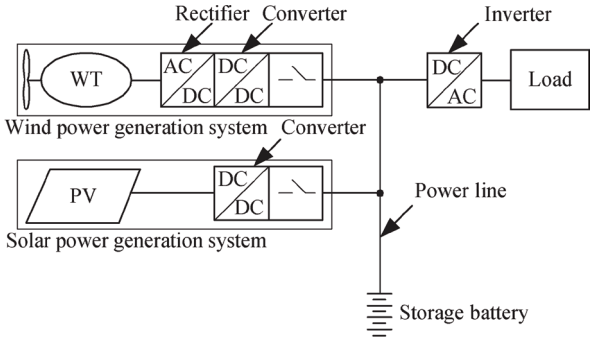

Fig. 1. Standalone hybrid wind-solar power generation system with central- ized inverter setup.

A dc–dc converter is mounted in both wind power and solar power generation systems. The two systems are inter-connected at the output sides of individual converters and are also connected to the storage battery. In such a configuration, each dc–dc converter is capable of monitoring the current and voltage of the storage battery, and optimally controlling battery charging, to supply power to the load [6]–[10]. In most cases where converters and storage batteries are set up at a centralized location, the storage batteries are commonly installed adjacent to the wind- and solar-power generation systems; therefore, there is generally no freedom to install

the batteries on flat ground or in places with good vehicular access for easy main- tenance and replacement.

In a hybrid system with a centralized inverter setup, as shown in Fig. 1, the output of dc–dc converters is sent to an external dc–ac inverter to supply ac power to load.

Therefore, a future increase in load will require an increase in inverter capacity [7]–[10]. In a system applying a dispersed inverter setup, as shown in Fig. 2, individual wind- and solar- power generation systems, each mounted with a dc–ac con- verter, are interconnected in parallel at the inverter output sides and are also connected to a diesel engine generator via a power line. At the same time, a dump load is also mounted on the same power line [11]–[13]. In this case, a storage battery is installed within the solar power generation system, and dump power iscontrolled as necessary to prevent battery overcharging. Several different techniques to prevent battery overcharging are widely used. For instance, the battery is installed adjacent to the wind-power generation system, and a solid-state relay or power de- vice is used as control switch of dump load [14]–[16]. Another technique is that surplus power is consumed by a hydrogen generator for a fuel battery instead of storage battery, and when the hydrogen tank becomes full, dump load is applied [17]. While these techniques construct a dispersed installation of different power sources, installation of dump load is necessary. Further, a dedicated high-speed line for battery current/voltage status data transmission, or otherwise a high-tech dump load control method, is necessary.

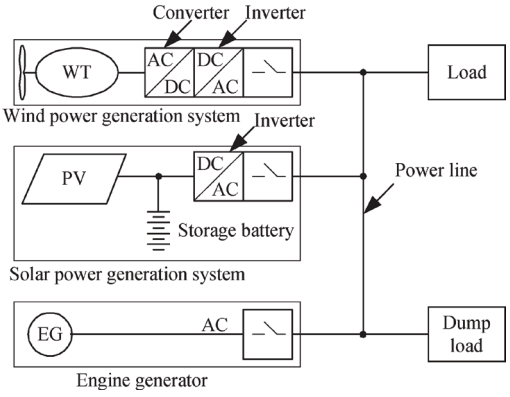

Fig. 1. Standalone hybrid wind-solar power generation system with central- ized inverter setup.

To resolve these problems, the authors have proposed a low- cost, standalone hybrid wind-solar power generation system applying advanced power control techniques. This system has the following features: 1) dispersed installation of different power sources that are interconnected in parallel; 2) elimi- nation of dump load by using a unique dump power control aimed at prevention of battery overcharging; 3) no need for dedicated high-speed line for battery current/ voltage status data transmission; and 4) easy capacity expansion through parallel connection of additional power sources to cope with future load increases.

Special attention has also been given to phased locked loop (PLL) control techniques. Through laboratory experiments, we investigated the behavior of current/voltage waves by inputting active-reactive power parameters into an experimental power control circuit and demonstrated a valid power control effect.

II. System Summary

A. System Configuration

The proposed standalone hybrid wind-solar power genera- tion system is, as shown in Fig. 3, in outline composed of four power sources: a wind power generation system (with a WT converter and a WT inverter), solar power generation system (with a PV inverter), storage battery (with a bidirec- tional inverter), and engine generator (EG); and a control unit. The control unit acts to send ON/ OFF operation commands to individual power sources and monitor power status via a simple communication line, which is all that is needed since the data traffic volume is small. Once an ON command is sent, each power source is autonomously operated via individual inverters; however, manual setting of inverter operating conditions is also possible if required. The inverters enable redundant parallel operation, making a reliable, stable power supply possible.

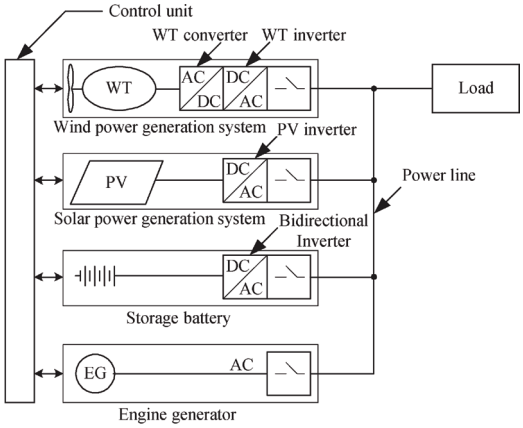

Fig. 3. Proposed standalone hybrid wind-solar power generation system.

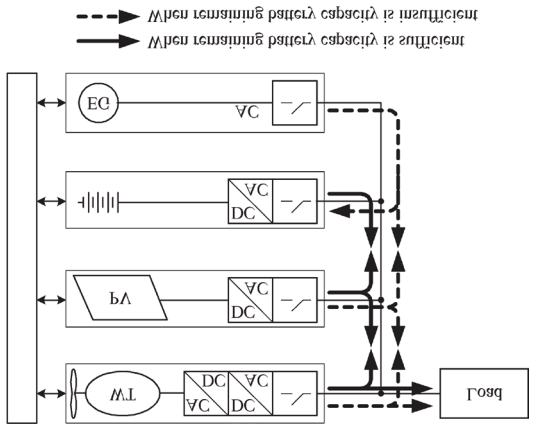

Fig. 4. System operation flow.

B. System Operation

Major operation flows of the proposed hybrid system, as shown in Fig. 4, are as follows.

1) When the remaining battery capacity is sufficient: EG op- eration stops, and all inverters operate in parallel. Power surplus and deficit according to the balance between the output and load can be optimally adjusted through battery charging or discharging.

2) When the remaining battery capacity is insufficient: EG and all inverters operate in parallel. When power generated by wind and solar power generation system is insufficient to meet load demand, EG compensates for the deficiency. Concurrently, EG charges the battery via the bidirectional inverter. This inverter regulates charging power for the battery so that EG can be operated at the optimal load factor congruent with high efficiency, following a command from the control unit.

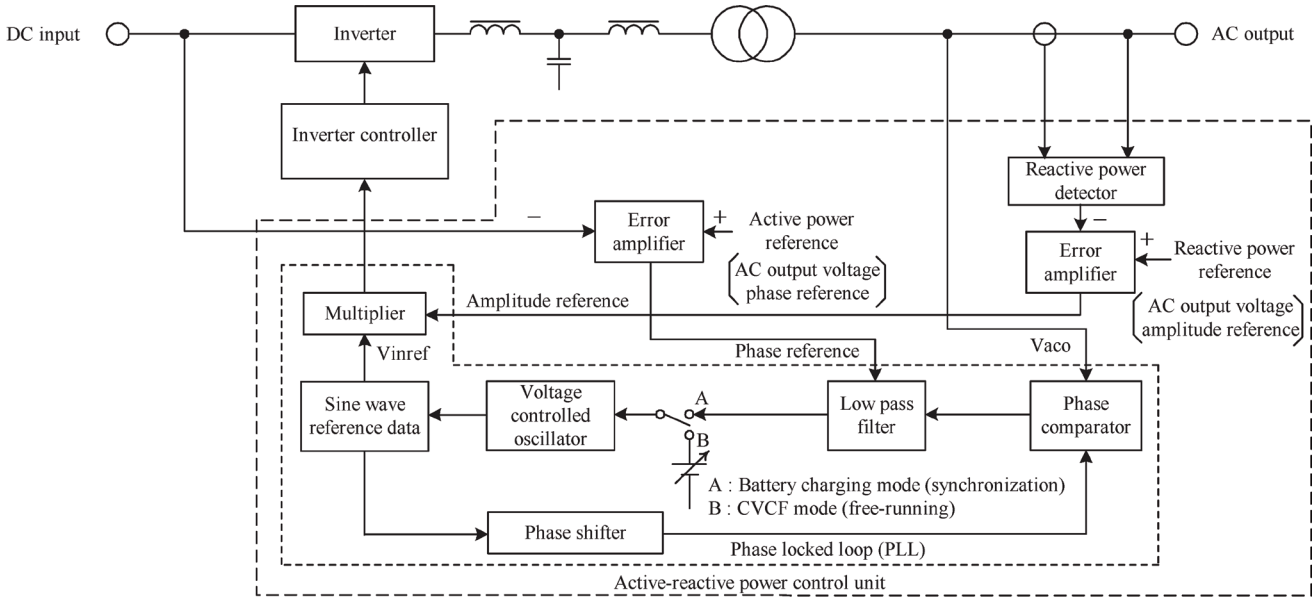

Fig. 5. Basic power control block diagram of inverter section.

III. System Pow E R Control Techniques

In the proposed hybrid system, we focused on how to control active-reactive power aiming at load sharing in parallel inverter operations, as well as how to control phase synchronization. Through our research activity, we devised an advanced dump power control technique without dump load.

A. Active-Reactive Power Control

Fig. 5 shows the basic power control block diagram for the inverter section. The auto-master-slave control technique is applied in all inverters. When EG is in operation, contactor A of each inverter is closed, and these contactors are in ac-synchronized operation with all inverters that act as slaves and with EG as master. When EG operation stops, contac- tor B of the storage battery bidirectional inverter is closed. This inverter functions as a master and is under the constant voltage constant frequency (CVCF) condition.

Contactor A of each remaining inverter acting as a slave is closed. Then, ac-synchronized operation will be underway. In studying the developmental concept of our proposed hybrid system, we fo- cused on the mechanism of the PLL in the active-reactive power control.

1) Phase Locked Loop (PLL): The PLL, which acts as a phase synchronization control, is composed of: a phase com- parator, low-pass filter, phase shifter, multiplier, and voltage- controlled oscillator (VCO). The phase comparator acts to multiply the ac output voltage wave by the cosine wave refer ence obtained from the sine wave reference passing through the phase shifter. The multiplied wave is converted to dc voltage for VCO frequency control via the low-pass filter. During synchronization with phase coincidence of the two waves (i.e., sine wave reference and ac output voltage wave), dc voltage becomes zero.

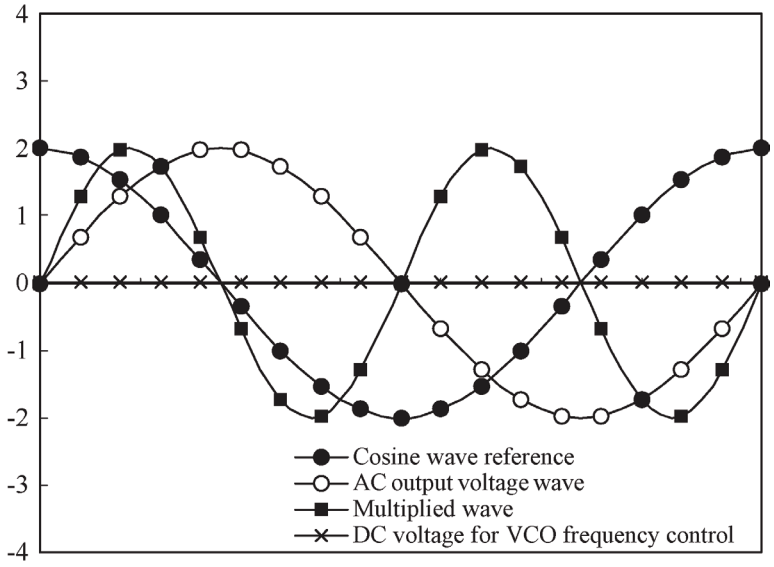

Fig. 6. Synchronization with phase coincidence

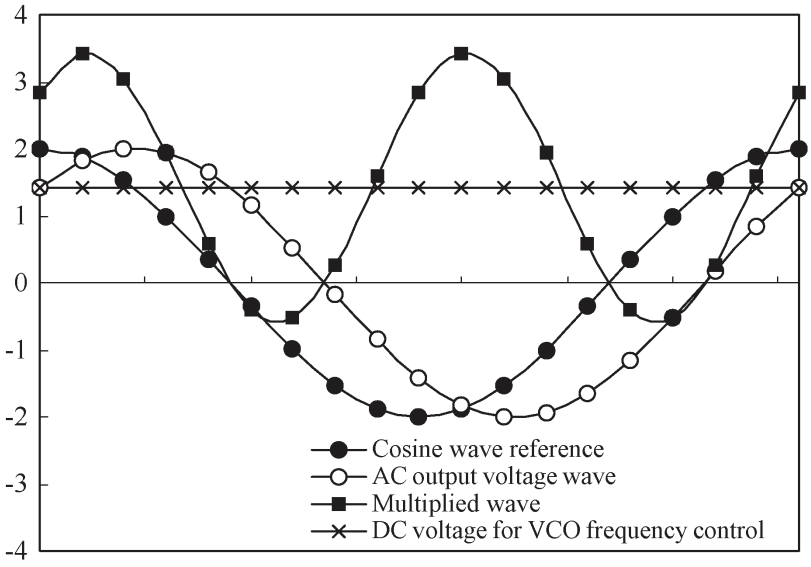

Fig. 7. Synchronization with phase shift.

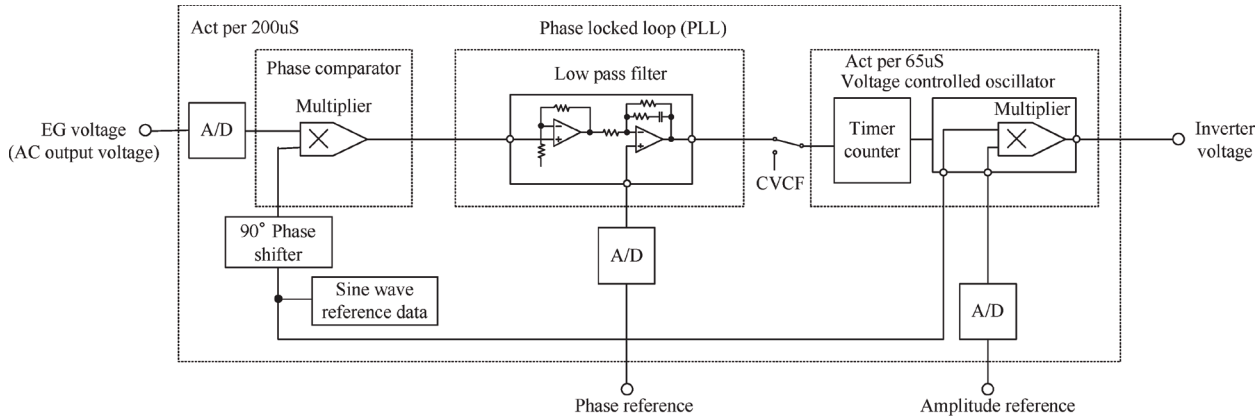

Fig. 8. Detail of PLL control block diagram

However, during synchronization with their phase shift, dc voltage does not become zero. Figs. 6 and 7 illustrate the individual waves and dc voltage for VCO frequency control when phase is coincident and shifted, respectively. The low-pass filter acts as an error amplifier. By giving an active power reference (i.e., ac output voltage phase reference) to the ampli- fier, the phase shift between sine wave reference and ac output voltage wave is adjusted while synchronization is maintained in a locked state. That is, active power control is possible by altering the dc voltage.

The dc voltage obtained through the low-pass filter is con- verted to the value of a timer counter by using the VCO. This value is defined as the duration for which the value obtained for a certain address in the sine wave reference data (256 addresses in total) is constantly output until the following address comes. In the case of 60 Hz, an address in the sine wave reference data is incremented by one at about every 65 μs. Synchronization is adjusted by changing the duration until the following address comes. The duration, or value of the timer counter, is updated about every 200 μs (i.e., about 65 μs × 3), that is, once per three addresses.

Fig. 8 shows the detail of the PLL control block diagram. Two elements, that is, the phase comparator output and the phase reference signal, are imported into the low-pass filter. The output of the phase comparator is imported as synchronization data (i.e., difference compared to reference frequency). The phase reference signal is imported as the amount of phase shifting in inverter output voltage while maintaining synchro- nization against voltage in the commercial power system. Thus, the active power varies along with the change in the phase reference signal.

For the reactive power, the sine wave reference regulated by VCO is multiplied with the signal in which the difference between reactive power reference and actual reactive power is amplified. The multiplied signal is defined as the control signal for inverter output voltage. By altering the reactive power reference (i.e., ac output voltage amplitude reference), reactive power control is made possible.

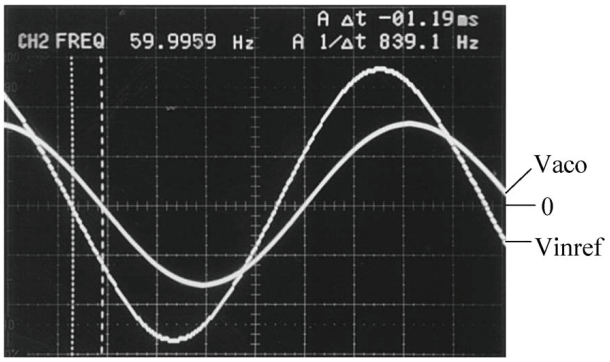

V_{aco}, V_{inref};1V/div., H:2ms/div.

Fig. 9. When Vaco becomes low (before correction) (phase difference: Ap- prox. 1.19 ms).

The PLL has a superior characteristic, in that synchronization is ensured even if the wave is deformed, especially when EG shows extreme voltage wave distortion. EG has a higher internal impedance, compared with the commercial ac line. Therefore, the output voltage of the EG has harmonic distortion when nonlinear loads such as switching elements, diodes and so forth are connected.

However, if the wave amplitude varies, the dc voltage ob- tained by passing through the low-pass filter also varies, giving rise to concern that output of active power may fluctuate.

Figs. 9 and 10 show voltage waves in the status in which the phase difference between sine wave reference and ac output voltage wave varies with increasing or decreasing amplitude of ac output voltage.

Fig. 11 shows the individual waves and dc voltage when ac output voltage becomes low, compared to that in Fig. 7, while maintaining the phase difference between the two waves. In this figure, it can be seen that the dc voltage became low.

To resolve this, we normalized the waves for which synchro- nization was required, and the normalized waves were input into the phase comparator, resulting in a stable output of active power. Corrected waves are shown in Figs. 12 and 13.

2) Operation of Parallel Inverters: We constructed a pro- totype standalone hybrid wind-solar power generation system, and conducted laboratory experiments.

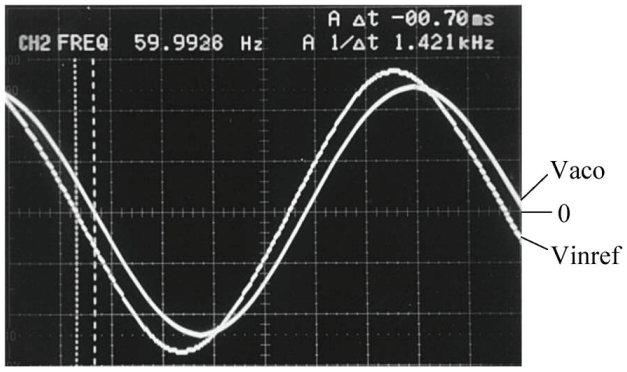

$V_{aco,}$ V_{inref};1V/div., H:2ms/div.

Fig. 10. When Vaco becomes high (before correction) (phase difference: Approx. 0.7 ms).

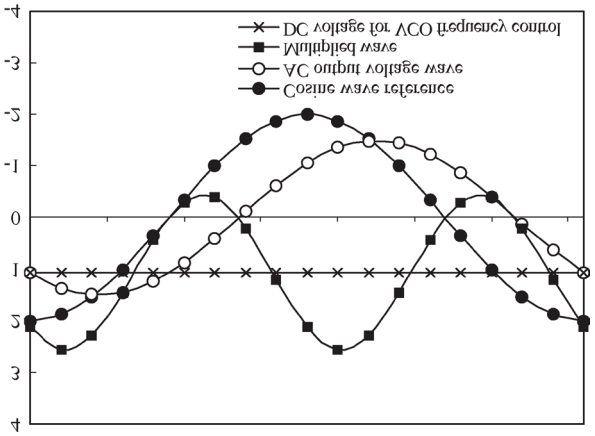

Fig. 11. When Vaco becomes low (computed values).

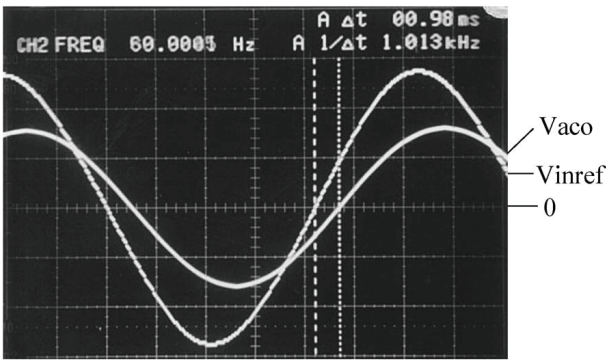

$V_{aco,}$ V_{inref};1V/div., H:2ms/div

Fig. 12. When Vaco becomes low (after normalization) (phase difference: Approx. 0.98 ms).

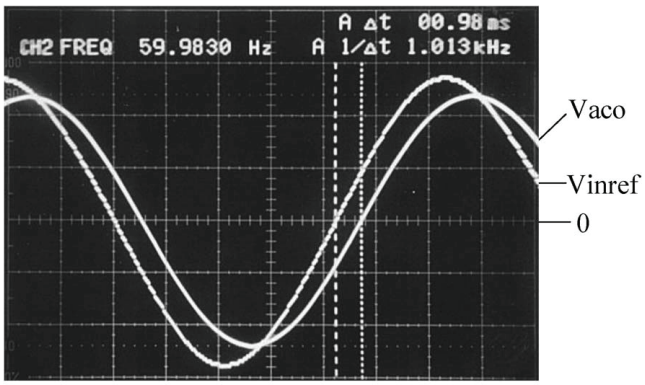

$V_{aco,}$ V_{inref};1V/div., H:2ms/div

Fig. 13. When Vaco becomes high (after normalization) (phase difference: Approx. 0.98 ms).

Table I shows the prototype specification of hybrid genera- tion system.

Fig. 14 shows an operating model of inverters in parallel. X_1, X_2, and X_3 are interconnected reactors installed in WT inverter, PV inverter, and Bidirectional inverter, respectively.

We conducted research into determination of optimal active power parameters for each inverter to regulate the out- put under the conditions that each inverter capacity was 3 kVA (with a power factor of 0.8), and the output voltage was single- phase 100 V 60 Hz. Where, active power is P_{sm} and reactive power is Q_{sm} at the sending-end; active power is P_{rm} and reactive power is Q_{rm} at the receiving-end; and the reactance of the interconnected reactor is X_m. Assuming that V_{sm} is defined as the sending-end voltage and V_r as the receiving-end voltage, and the angle of phase difference is δ, each of P_{sm} , Q_{sm} , P_{rm} , and Q_{rm} is represented as follows [18], [19]:

$$P_{sm} = P_{rm} = \frac{V_{sm}V_r}{X_m} SIN\delta \quad (1)$$

$$Q_{sm} = \frac{V_{sm}^2 - V_{sm}V_r COS\delta}{X_m} \quad (2)$$

$$V \quad V \; COS\delta - V^2$$

$$Q_{rm} = \frac{sm \quad rr}{X_m} \quad (3)$$

TABLE I SPECIFI CATION OF PROTOT
Y P E HYBRID GENERAT ION SYSTEM

Specification of Wind Power Generation System	
Item	Specification
Wind Turbine	
1) Output Capacity	3.5kW
2) Output Voltage	3-phase 3-wire AC100V
AC-DC Converter	
1) Output Capacity	3.5kW
2) Output Voltage	DC250V
DC-AC Inverter	
1) Output Capacity	3kW
2) Output Voltage	1-phase 2-wire AC100V Power factor 0.8
Solar Power Generation System	
Item	Specification
Solar Panel	
1) Output Capacity	3.1kW
2) Open Circuit Voltage	DC344V
DC-AC Inverter	
1) Output Capacity	3kW
2) Output Voltage	1-phase 2-wire AC100V Power factor 0.8
Storage Battery System	
Item	Specification
Storage Battery Module	
1) Rated Voltage	DC12V
2) Rated Capacity	24Ah
Storage Battery Unit	
1) Rated Voltage	DC288V
2) Rated Charging Voltage	DC332.1V
3) Rated Charging Current	DC10A
4) Connection	24 modules connected in series in two parallel
DC-AC Bidirectional Inverter	
1) Output Capacity	3kW
2) Output Voltage	1-phase 2-wire AC100V Power factor 0.8
Engine Generator	
Item	Specification
1) Output Capacity	10kVA
2) Output Voltage	1-phase 2-wire AC100V Power factor 0.8

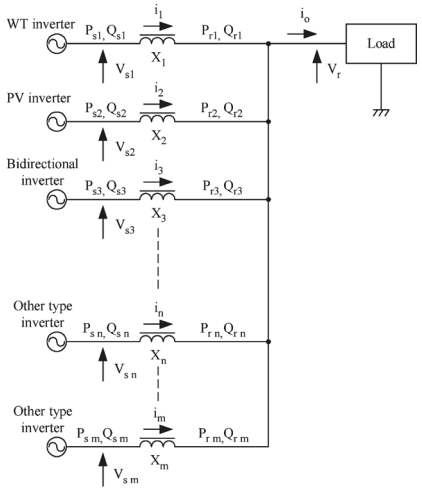

Fig. 14. Operating model of parallel inverters.

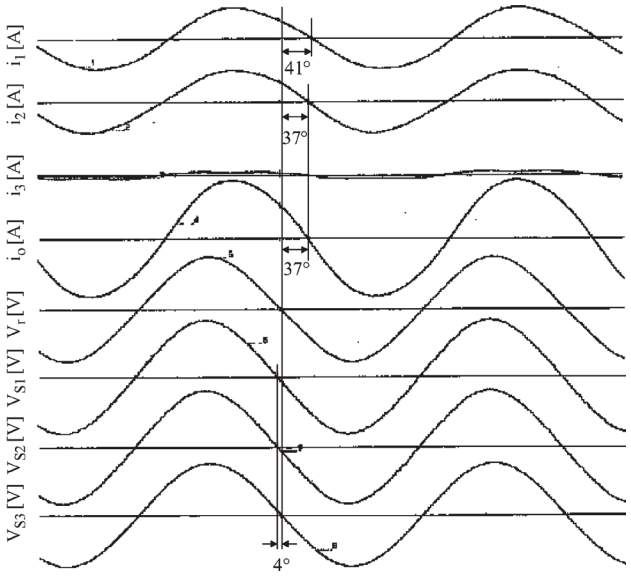

Fig. 15. Current and voltage waves of each inverter mounted in system prototype.

Here, *m* indicates the number of power sources that are operated in parallel. It is desirable to regulate the voltage amplitude difference and the angle of phase difference to be within the ranges from 5 V to 15 V, and from 5° to 10°, respectively, based on the characteristics of the active-reactive power control unit as shown in Fig. 3. When δ is 7.5° and Vr is 100 V, V_{sm} becomes 109 V by using (1) and (2). The reactance of the interconnected reactor becomes 1.57 mH.

Fig. 15 shows the current and voltage waves of each inverter mounted in the prototype. 50% of active power was supplied tothe load by individual WT and PV inverters, under the condition that the reactive power of the storage battery bidirectional inverter became zero. The capacity of load was 3 kVA, and the power factor was 0.8.

From individual waves shown in Fig. 15 and results of the measured output voltage and output current of each inverter, as shown in Table II, several observations are worthy of remark. For the bidirectional inverter, the output voltage phase showed greater coincidence with amplitude, as compared to load volt- age, and only a little output current flow was caused. For the WT and PV inverters, output voltage phase advanced 4° and voltage amplitude became about 8 V to 10 V higher as com- pared with load voltage, and an output current flow of 16.1 A from each inverter was seen. These observations show that the WT and PV inverters each supply about 12 A to 13 A of the active current and about 9 A to 11 A of the reactive current to the load consumed.

There was good agreement between theoretical and mea- sured values, when the loss of output transformers and their leakage inductances were neglected. It was confirmed that each inverter controls the output power under optimal conditions by reactive power control (i.e., amplitude control) and active power control (i.e., phase control).

The current phase of WT inverter was 41° , with 4° lag compared to other inverters. This was because some circulating current flowed to each inverter through WT inverter since voltage of WT inverter was higher than those of other inverters. Fig. 15 indicates slight deformations of inverter output cur- rent waves. This is because the output current was controlled so that the inverter output voltage can have a clear sine wave since inverter control was done with the voltage control method in which current is controlled with a minor loop mechanism. Thus, the inverter output voltage has clear sine waves, although the output current does not have constant clear sine waves.

Fig. 16 shows charging current and voltage characteristics of storage battery, and Fig. 17 shows the bidirectional inverter voltage waves in slave mode, showing that the charging was done under the constant voltage constant current condition.

The rating of each lead-acid battery module was 12 V, 24 Ah. The battery unit was comprised of 24 battery modules con- nected in series in two parallel rows. Floating charging voltage was set as 331.2 V, and charging current was set at about 10 A.

B. Dump Power Control

Following research into active-reactive power control tech- niques, we endeavored to devise effective control of dump power. When either wind power or solar power generation becomes greater than load, EG stops, and the bidirectional inverter as a master is operated under the CVCF condition. Then, dump power, which is defined as the surplus portion obtained after deducting load from generated power, is used as charging power for storage battery. In the course of battery charging, an advanced technique to prevent battery overcharge is required. Dump load (e.g., a resistor load or radiator), which functions to consume dump power, is conventionally mounted in parallel with the battery or ac output point, as shown in Fig. 18 [11]–[13].

TABLE II MEASURED OUTPUT VOLTAGE AND CURRENT OF EAC H INVERTER

	Voltage		Apparent current		Active current	Reactive current
	Amplitude	Phase	Amplitude	Phase		
Bidirectional inverter	100V (100V)	0° (0°)	1.3A (0A)	37° (0°)	1.0 (0A)	0.6 (0A)
WT inverter	109.7V (105.6V)	4° (3.86°)	16.1A (15A)	41° (36.9°)	12.2A (12A)	10.6A (9A)
PV inverter	108.1V (105.6V)	4° (3.86°)	16.1A (15A)	37° (36.9°)	12.9A (12A)	9.7A (9A)
Load	100V (100V)	0° (0°)	30.9A (30A)	37° (36.9°)	24.7A (24A)	18.5A (18A)

Figures in parentheses are theoretical values.

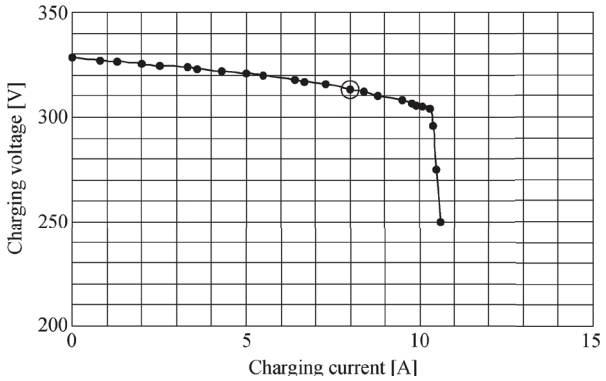

Fig. 16. Charging current and voltage characteristics of the storage battery.

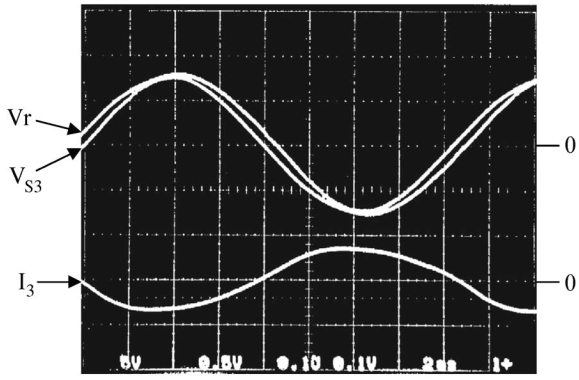

Vr, VS3;100V/div., i3:50A/div., H:2ms/div

Fig. 17. Waveforms of the bidirectional inverter at the charging current 8 A (black circled in Fig. 16).

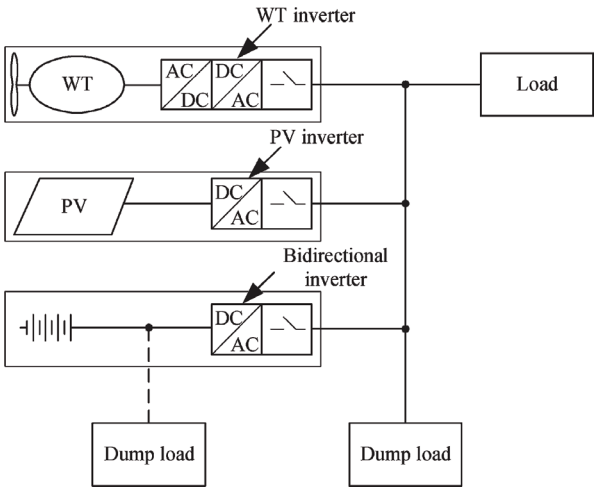

Fig. 18. Conventional dump power control technique.

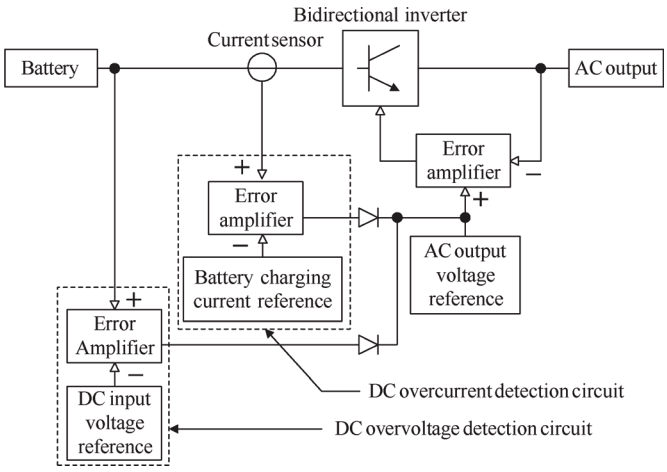

Fig. 19. Dump power control block diagram of bidirectional inverter.

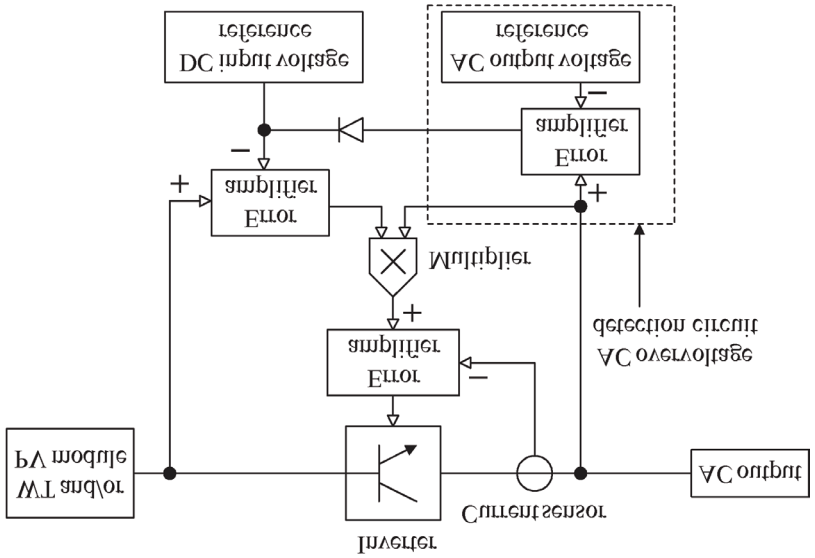

Fig. 20. Dump power control block diagram of WT and PV inverters.

However, since dump power varies continuously, it is dif- ficult to regulate dump load by simply inputting dump load, because this hinders flexible control of battery charging. To stabilize both charging current and charging voltage of storage battery, we developed a unique advanced dump power control technique characterized by dump power regulation without any dump load. This technique allows for quick response to fluctuating dump power as well as reduction of needless dump power control, contributing to more effective use of natural energy.

1) Dump Power Control Technique: Figs. 19 and 20 show the dump power control block diagram of the bidirectional inverter and that of the WT and PV inverters, respectively. Also, Fig. 21 shows the flowchart of the dump power control.

When there is no dump power, the inverter acts only with ac output voltage reference. In Fig. 19, in case the larger of the outputs from dc overcurrent detection circuit and dc overvolt- age detection circuit exceeds the ac output voltage reference, the diode related to the error amplifier with the larger output is turned on. Then, dc overcurrent value or dc overvoltage value is added to the ac output

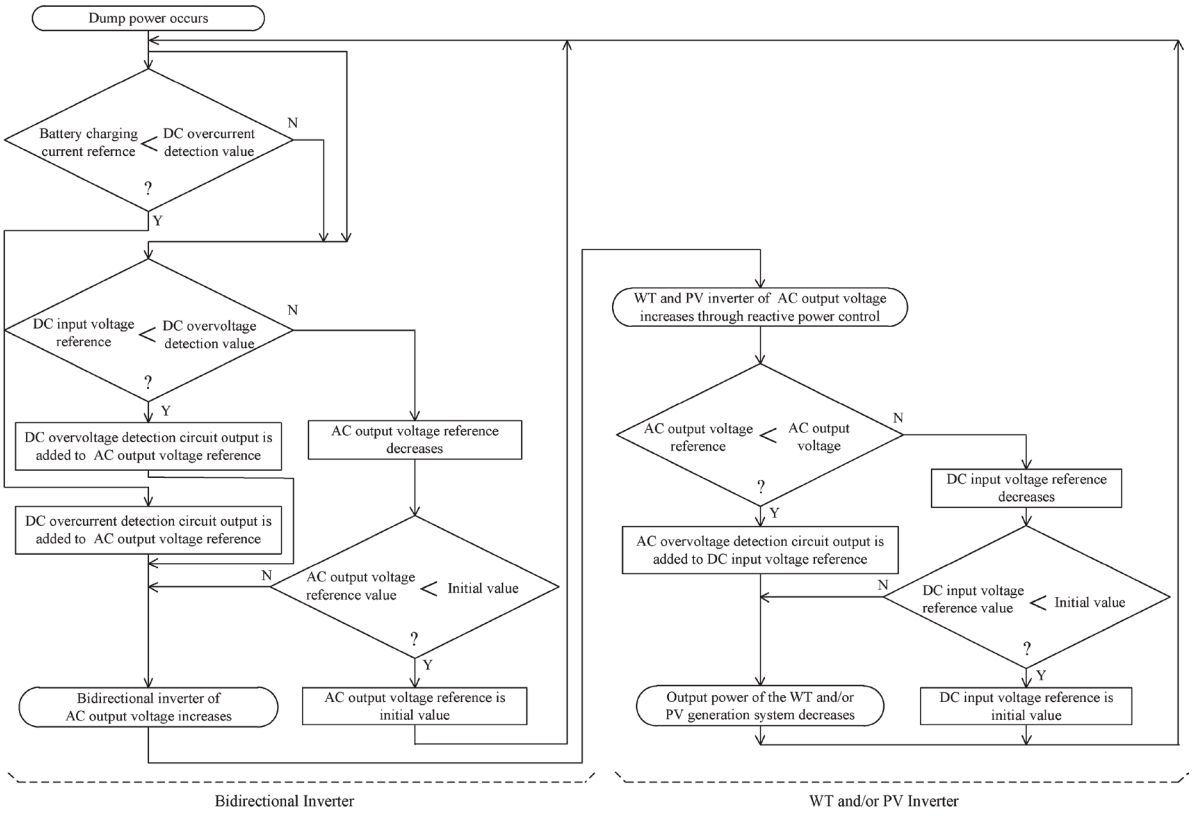

Fig. 21. Flowchart of the dump power control.

voltage reference; thus, the inverter acts. In contrast, in Fig. 20, in case the output from ac overvoltage detection circuit exceeds the dc input voltage reference, the diode related to the error amplifier is turned on. Then, ac overvoltage value is added to the dc input voltage reference; thus, the inverter acts.

Specifically, when dump power occurs, the surplus portion flows into the storage battery through the bidirectional inverter. Charging current flowing into the battery is detected by the current sensor. When the battery current exceeds the charging current reference, the difference is amplified and added to the ac output voltage reference. While, when the battery voltage exceeds the charging voltage reference, the difference is ampli- fied and added to the ac output voltage reference. Thus, as the ac output voltage reference increases, the output voltage of the bidirectional inverter also increases. When the output voltage of the bidirectional inverter increases, the output voltages of WT and PV inverters increase through reactive power control.

If the output voltage becomes greater than the ac output voltage reference, the difference is amplified and added to the dc input voltage reference. With this, the phase reference as shown in Fig. 8 varies, allowing the PLL to control inverter voltage phase. Because the output voltages of the WT and PV inverters are designed to be controlled by the dc input voltage reference, the ac output voltage decreases as the dc input voltage reference increases. In this way, a feedback loop is formed in the proposed system. Dump power is controlled; and charging current and charging voltage in the storage battery can be stabilized. The dump power control technique developed can be summarized as follows:

1) dump load can be eliminated;

2) effective dump power control without dump load to prevent battery overcharging is possible, contributing to extended battery life;

3) since dump power data is interactively exchanged through the power line, a private communication line between different power sources is unnecessary, resulting in a simple hybrid system arrangement.

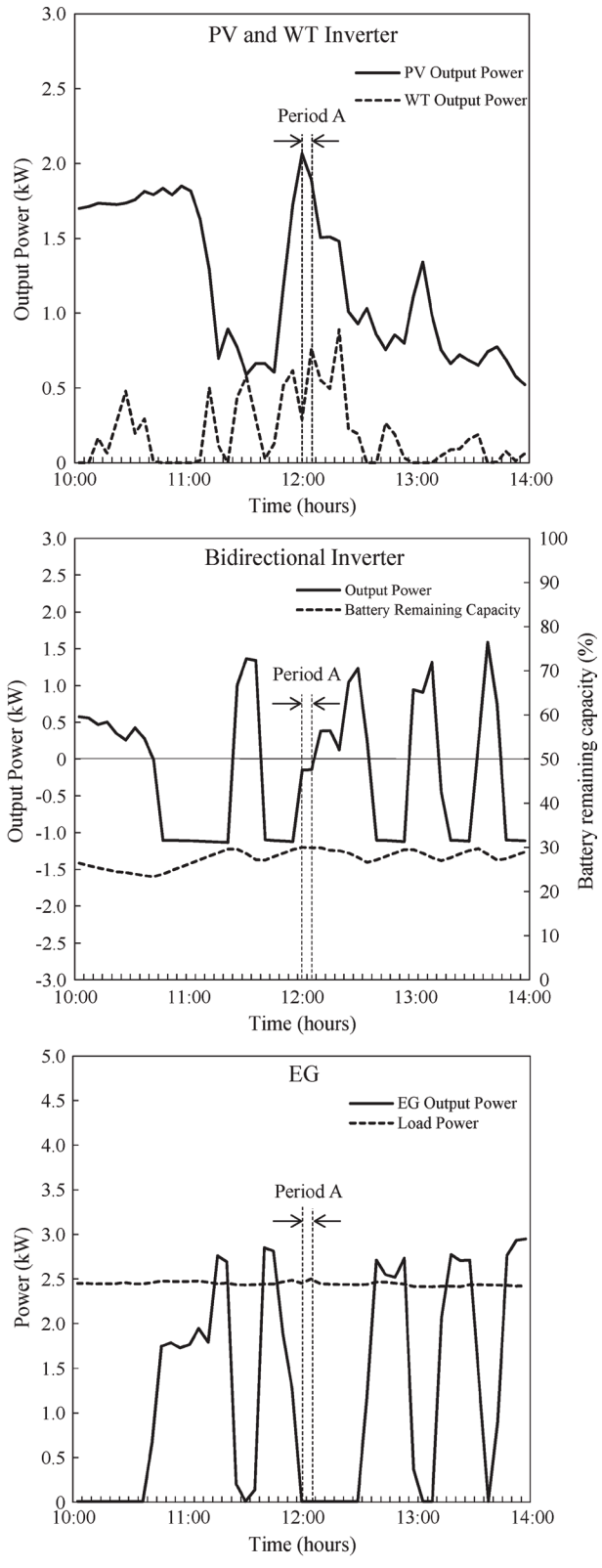

Fig. 22. Field test results of the dump power control.

2) Experimental Results of Dump Power Control: We carried out a field test of the proposed hybrid wind-solar power generation system to get data on the output power, load power, and battery remaining capacity of individual power generation systems. Fig. 22 shows such data from 10:00 to 14:00 on a day when dump power occurred. In this test, EG started when battery remaining capacity fell to about 25% or below, and EG stopped when capacity exceeded about 30%. The output power of the bidirectional inverter was positive during discharge and negative during charge.

"Period A" indicated in this figure shows a period during which dump power controller worked. In the period, EG did not operate, and dump power occurred because power generated by PV and WT exceeded power consumption. The fact that the bidirectional inverter had negative output power during this period shows that the battery was charged. It can be seen in Fig. 22 that dump power controller worked since the battery kept its charging power constant.

IV. Conclusion

The authors have proposed a unique standalone hybrid wind- solar power generation system, which is characterized by PLL control and dump power control. In particular, dump power control allows for formation of a feedback loop in this system, meaning that there is no requirement for a dedicated high-speed line to transmit storage battery voltage and current data. In case the power line is used as a media for data transmission, the line voltage amplitudes can be applied as a means of data transmission; thus, there is no requirement for installation of any optical fiber transmission line or power line carrier system through which harmonic signals are applied to power line. In addition, neither dump load nor dump load control device are necessary. Under our dump power control, regulation of output is done without battery overcharging, and effective use of surplus power is made possible. This contributes to battery life extension and realization of a low-cost system. The system, through ac system interconnection, will also allow flexible sys- tem expansion in the future. Further, power sources including EG can be flexibly interconnected anywhere through the same power line, and power quality stability can be maintained by controlling the phase and amplitude of ac output voltage. It is expected that this hybrid system into which natural energy is incorporated, and which makes use of various power control techniques, will be applicable in rural locations, even those with poor communications media.

The system will also contribute to global environmental protection through application on isolated islands without any dependence on commercial power systems.

References

[1] S.-K. Kim, J.-H. Jeon, C.-H. Cho, J.-B. Ahn, and S.-H. Kwon, "Dynamic modeling and control of a grid-connected hybrid generation system with versatile power transfer," *IEEE Trans. Ind. Electron.,* vol. 55, no. 4, pp. 1677–1688, Apr. 2008.

[2] K. Kobayashi, H. Matsuo, and Y. Sekine, "An excellent operating point tracker of the solar-cell power supply system," *IEEE Trans. Ind. Electron.,* vol. 53, no. 2, pp. 495–499, Apr. 2006.

[3] K. Kobayashi, H. Matsuo, and Y. Sekine, "Novel solar-cell power supply system using a multiple-input dc–dc converter," *IEEE Trans. Ind. Elec- tron.,* vol. 53, no. 1, pp. 281–286, Feb. 2006.

[4] A. I. Bratcu, I. Munteau, S. Bacha, D. Picault, and B. Raison, "Cascaded dc–dc converter photovoltaic systems: Power optimization issues," *IEEE Trans. Ind. Electron.,* vol. 58, no. 2, pp. 403–411, Feb. 2011.

[5] W. Li, G. Joos, and J. Belanger, "Real-time simulation of a wind turbine generator coupled with a battery supercapacitor energy storage system," *IEEE Trans. Ind. Electron.,* vol. 57, no. 4, pp. 1137–1145, Apr. 2010.

[6] F. Valenciaga and P. F. Puleston, "Supervisor control for a stand-alone hybrid generation system using wind and photovoltaic energy," *IEEE Trans. Energy Convers.,* vol. 20, no. 2, pp. 398–405, Jun. 2005.

[7] S. Meenakshi, K. Rajambal, C. Chellamuthu, and S. Elangovan, "Intelli- gent controller for a stand-alone hybrid generation system," in *Proc. IEEE Power India Conf.,* New Delhi, India, 2006.

[8] R. Belfkira, O. Hajji, C. Nichita, and G. Barakat, "Optimal sizing of stand-alone hybrid wind/pv system with battery storage," *in Proc. Power Electron.* Appl. Eur. Conf., Sep. 2007, pp. 1–10.

[9] S. Wang and Z. Qi, "Coordination control of energy management for stand-alone wind/pv hybrid systems," *in Proc. IEEE ICIEA,* May 2009, pp. 3240–3244.

[10] C. Liu, K. T. Chau, and X. Zhang, "An efficient wind-photovoltaic hy- brid generation system using doubly excited permanent- magnet brush-less machine," *IEEE Trans. Ind. Electron.,* vol. 57, no. 3, pp. 831–839, Mar. 2010.

[11] F. Bonanno, A. Consoli, S. Lombardo, and A. Raciti, "A logistical model for performance evaluations of hybrid generation systems," *IEEE Trans. Ind. Appl.,* vol. 34, no. 6, pp. 1397–1403, Nov./Dec. 1998.

[12] M. H. Nehrir, B. J. LaMeres, G. Venkataramanan, V. Gerez, and L. A. Alvarado, "An approach to evaluate the general performance of stand-alone wind/photovoltaic generating systems," *IEEE Trans. Energy Convers.,* vol. 15, no. 4, pp. 433–439, Dec. 2000.

[13] J. M. Carrasco, L. G. Franquelo, J. T. Bialasiewicz, E. Galvan, R. C. P. Guisado, M. A. M. Prats, J. I. Leon, and N. Moreno-Alfonso, "Power-electronic systems for the grid integration of renewable energy sources: A survey," *IEEE Trans. Ind. Electron.,* vol. 53, no. 4, pp. 1002–1016, Jun. 2006.

[14] S. Jiao, G. Hunter, V. Ramsden, and D. Patterson, "Control system design for a 20 kW wind turbine generator with a boost converter and battery bank load," *in Proc.* PESC, Sep./Oct. 2001, pp. 2203–2206.

[15] S. Tanezaki, T. Matsushima, and S. Muroyama, "Stand-alone hybrid power supply system composed of wind turbines and photovoltaicmodules for powering radio relay stations," *in Proc. IEEE INTELEC,* Oct. 2003, pp. 457–462.

[16] A. M. O. Haruni, A. Gargoom, M. E. Haque, and M. Negnevitsky, "Dy- namic operation and control of a hybrid wind-diesel stand alone power systems," in Proc. IEEE APEC, Feb. 2010, pp. 162–169.

[17] D. B. Nelson, M. H. Nehrir, and C. Wang, "Unit sizing of stand-alone hybrid wind/pv/fuel cell power generation systems," in Proc. *IEEE Power Eng. General Soc. Meeting,* Jun. 2005, vol. 3, pp. 2116–2122.

[18] M. C. Chandorkar, D. M. Divan, and R. Adapa, "Control of parallel connected inverters in standalone ac supply systems," *IEEE Trans. Ind. Appl.,* vol. 29, no. 1, pp. 136–143, Jan./Feb. 1993.

[19] J. M. Guerrero, J. Matas, L. G. de Vicuna, M. Castilla, and J. Miret, "Wireless-control strategy for parallel operation of distributed-generation inverters," *IEEE Trans. Ind. Electron.,* vol. 53, no. 5, pp. 1461–1470, Oct. 2006.